

# CMOS Magnetic Sensors for Wearable Magnetomyography

Hadi Heidari, *Senior Member, IEEE*, Siming Zuo, Agamemnon Krasoulis, *Member, IEEE*, and  
Kianoush Nazarpour, *Senior Member, IEEE*

**Abstract**— Magnetomyography utilizes magnetic sensors to record small magnetic fields produced by the electrical activity of muscles, which also gives rise to the electromyogram (EMG) signal typically recorded with surface electrodes. Detection and recording of these small fields requires sensitive magnetic sensors possibly equipped with a CMOS readout system. This paper presents a highly sensitive Hall sensor fabricated in a standard  $0.18\ \mu\text{m}$  CMOS technology for future low-field MMG applications. Compared with previous works, our experimental results show that the proposed Hall sensor achieves a higher current mode sensitivity of approximately  $2400\ \text{V/A/mT}$ . Further refinement is required to enable measurement of MMG signals from muscles.

## I. INTRODUCTION

Electromyography (EMG) is a method by which the electrical activity of the skeletal muscles is recorded. Magnetomyography (MMG) is the measurement of the magnetic signal, generated when the muscle is contracted [1-2]. The correspondence between these two techniques stems directly from the Maxwell-Ampère law which states that time-changing electrical current densities generate a magnetic field. There are many advantages of using MMG instead of EMG. Firstly, MMG provides a higher signal-to-noise ratio than the EMG [3], and thus can offer a comprehensive measurement of muscle activity from deeper muscles without using an invasive measurement technique. Moreover, electric fields are affected by the presence of various layers of tissues between the skin surface and source besides the DC and noise voltages generated at the skin-electrode interface, whereas these tissues are in reality a way open to the magnetic fields [4]. Whilst EMG has been used widely in clinical practice, the use of MMG has been very limited [1]. This is mainly because the magnitude of the EMG signal is in the scale of milli-volts and that for the

AK was supported in part by grants EP/F500386/1 and BB/F529254/1 for the University of Edinburgh, School of Informatics Doctoral Training Centre in Neuroinformatics and Computational Neuroscience from the UK Engineering and Physical Sciences Research Council (EPSRC), UK and Biotechnology and Biological Sciences Research Council (BBSRC), and the UK Medical Research Council (MRC). KN is supported by the EPSRC grant EP/R004242/1. HH is supported by the Royal Society grant RSG/R1/180269.

HH and SZ are with the Microelectronics Lab, School of Engineering, University of Glasgow, Glasgow, G12 8QQ, UK ([hadi.heidari@glasgow.ac.uk](mailto:hadi.heidari@glasgow.ac.uk)).

AK is with School of Engineering, Newcastle University, Newcastle-upon-Tyne, NE1 7RU, UK (e-mail: [agamemnon.krasoulis@gmail.com](mailto:agamemnon.krasoulis@gmail.com)).

KN is with School of Engineering and Institute of Neuroscience, Newcastle University, Newcastle-upon-Tyne, NE1 7RU, UK (e-mail: [kianoush.nazarpour@newcastle.ac.uk](mailto:kianoush.nazarpour@newcastle.ac.uk)).

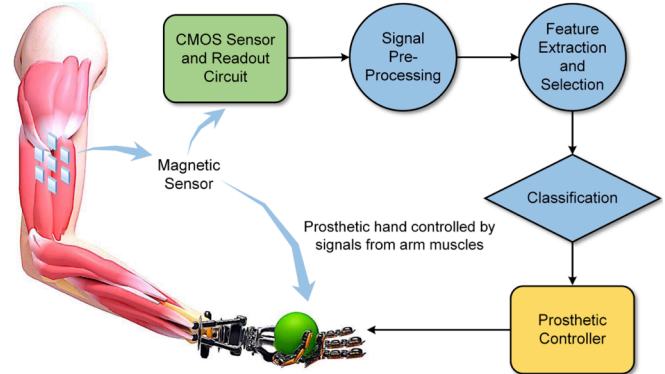


**Fig. 1.** Wearable and implantable magnetomyography for prosthesis control—a vision.

MMG signal is in the scale of pico ( $10^{-12}$ ) to femto ( $10^{-15}$ ) Tesla (T) [1], depending upon measurement conditions and whether the MMG sensors are to be implanted in the muscle, implanted below the skin or applied on the skin outside of the body. In fact, another advantage of MMG over EMG comes from the vectorial nature of the magnetic field. Such vector information could aid in recording movements of skeletal muscles, while the surface-recorded EMG is restricted to the plane of the skin and yields no such vector information [3].

Common magnetic sensors based on the magneto-resistive [e.g. anisotropic magnetoresistance (AMR), giant magnetoresistance (GMR), tunnel magnetoresistance (TMR) sensors, the fluxgate effect and giant magneto-impedance (MI) effect], have been studied intensively over the past few years. These sensing modalities have also been extensively utilized in medical and biological applications [5]. However, there are drawbacks to these proposed technologies. They are not compatible with CMOS technology and low power requirements. For instance, a low-field AMR sensor needs integrated setting and resetting current pulses with several hundred milliamperes; the integrated fluxgate sensor requires strong operating currents to drive the open-loop core into saturation; For magnetic field sensors containing ferromagnetic materials, the offset of the sensor changes after exposure to a high magnetic field.

The typical tested technique to record magnetic fields in the femto Tesla range is the use of superconducting quantum interference devices (SQUID), which are typically used to measure and localize the brain activity [1], [6]. Nevertheless, the SQUID technology requires magnetic-shield room and refrigeration system. Therefore, the SQUID systems are expensive and bulky for personal daily use.

To miniaturize the magnetic detection device, we designed a single-chip based on the Hall Sensor for Wearable Magnetomyography, as shown in Fig. 1. The proposed Hall sensor is low cost, the chip is small in size, and features low power consumption. The standard CMOS technology allows for integrating state-of-the-art op-Amp, integrator, and a digital block. As our target is to use a standard CMOS technology, the choice for integrated magnetic sensors is clearly limited to silicon Hall elements. The results show a Hall-element sensitivity of 2400 V/A/mT and a biasing current of 12  $\mu$ A with total power consumption of 120  $\mu$ W.

## II. MMG FOR UPPER-LIMB PROSTHESIS CONTROL

The loss of any limb, particularly the hand, affects an individual's quality of life profoundly. An artificial arm, or prosthesis, is an example of technology that can be used to help a person with limb difference to perform essential activities of daily living. Prosthetic hands are often controlled by sensing the muscle contractions of the remaining arm to which the prosthesis is attached, allowing the user to operate the prosthesis by flexing their muscles. These prostheses are in fact controlled by the EMG signals that are recorded non-invasively from the skin surface of an amputee's stump.

Decoding movement intentions using the surface EMG signals is a challenging machine learning problem. Outside clinic and during ordinary prosthesis use, this is exacerbated due to physical displacement of the surface electrodes because of donning and doffing and natural movement of the residual muscles under the skin with respect to surface electrodes. Due to these challenges, academic research in microsystems has moved towards wearable and implantable EMG electrodes, which are currently commercially available, e.g. from Ripple Ltd., USA.

We have recently shown that magnetometry data recorded during muscle function with off-the-shelf inertial measurement units (IMUs) (range  $\pm 1$  mT) placed on the skin surface can be used to control a hand prosthesis in real-time [7]. We concluded that measuring the magnetic field around the muscle area could indirectly provide an alternative measurement of muscular activity. A model of the magnetic fields created by single motor unit compound action potentials in skeletal muscle is shown in [3]. In this study, we present the circuit design scheme of a micro-Hall sensor with potential applications in wearable and implantable MMG. This paper is organized as follows: Section III describes the

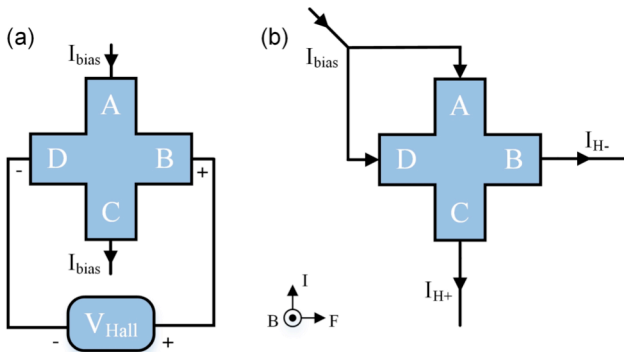


**Fig. 2.** The Hall plate operating in (a) the voltage- and (b) the current-modes.

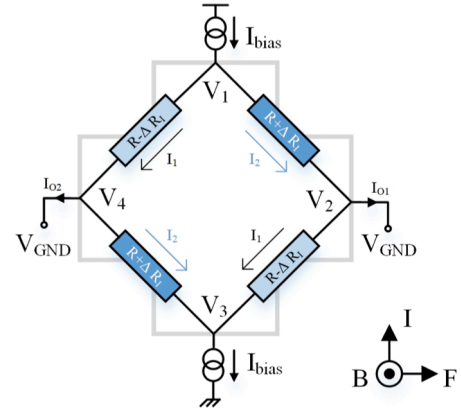


**Fig. 3.** A cross-shaped Hall plate: a Wheatstone bridge model of cross-shape Hall sensor in the current-mode configuration.

design of CMOS Hall sensors. Section IV reports simulation results and the comparison between our model and previously reported experimental data. Section V concludes this paper.

## III. DESIGN OF THE CMOS HALL SENSORS

A magnetic Hall sensor is a transducer, which converts a magnetic field to a corresponding electrical signal, either voltage or current, and is divided into voltage-mode and current-mode operations. For both modes, the biasing provides a constant voltage or a constant current. In the voltage-mode, as shown in Fig. 2(a), the magnetic field (orthogonal to the Hall plate) is converted into an output voltage. However, nowadays the current-mode is an alternative to the widely used voltage-mode for two reasons. Firstly, the layout permits current spinning [8], a technique which is used to compensate for the offset and then provides a differential current as an output signal. In addition, by employing the concept of a Wheatstone bridge model of cross-shape Hall sensors, the sensitivity in the current-mode with an equal change of the resistors is twice larger than the voltage-mode [8]. This configuration is shown in Fig. 2(b). This design optimizes our previous sensors in [9], [10] to obtain higher sensitivity and lower power consumption for magnetomyography applications.

In the current-mode operation, a bias current is utilized on the sensing terminals which are kept at the same voltage in the absence of an external magnetic field. When an external magnetic field is applied to the Hall sensor, a differential current is appeared on the sensing terminals. This is called the *Hall current*, and from the materials and shape, it is defined as

$$I_{Hall} = \mu_H \frac{w}{l} B I_{bias}, \quad (1)$$

where  $\mu_H$  and  $\frac{w}{l}$  refer the Hall mobility of majority carriers and width-to-length ratio of the sensor plate, respectively. In both modes, signal to noise ratio (SNR) and offset are two key criteria for performance evaluation. Several techniques have been developed to improve these characteristics [11].

Eq. (1) can also be used to define the sensitivity of the sensor, which reflects the capability of the sensor to translate the magnetic field into a Hall current. The sensitivity  $S_{A_I}$  relating the current output quantity is defined as [11]

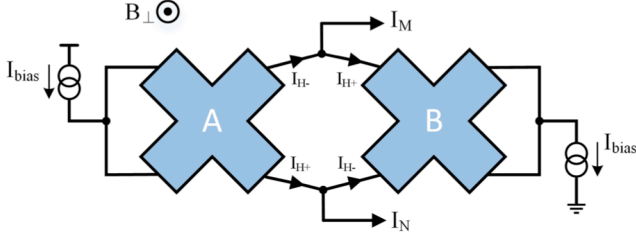


**Fig. 4.** The structure of the proposed twin cross-shaped Hall sensor.

$$S_{A_I} = \frac{I_{Hall}}{B} \text{ [A/T]}. \quad (2)$$

In addition, the relative sensitivity  $S_I$  can be obtained by including the bias quantity of the denominator of Eq. (2). The current-mode sensitivity is therefore [11] as follows

$$S_I = \left| \frac{I_{Hall}}{I_{bias} \times B} \right| \text{ [T}^{-1}\text{]}. \quad (3)$$

The applied magnetic field changes the current flow in the body sensor and this eventually produces an increment in the variation of the sheet-to-body resistance in the device. The sensor model as a bridge of resistances is shown in Fig. 3. Four resistors model the DC electrical relationship between the input and output nodes. The value of resistors is changed by  $\Delta R_I$  due to the applied magnetic field.

Since the current-mode and voltage-mode operations express different boundary conditions, the current-mode is affected differently by the magnetic field in the device and, therefore, the bridge resistors are varied. For the current-mode Hall sensors (Fig. 3) a bias current is injected into a terminal ( $V_1$ ) of the Hall plate, and the same bias current is obtained from opposite terminal ( $V_3$ ). The output terminals ( $V_2$  and  $V_4$ ) are at the same ground voltage. The differential output currents are given by

$$I_1 = \frac{V_1}{R - \Delta R_I}, \quad (4)$$

$$I_2 = \frac{V_1}{R + \Delta R_I}. \quad (5)$$

Therefore, the differential Hall current is expressed as

$$I_{Hall} = 2I_{bias} \frac{\Delta R_I}{R} \quad (6)$$

Fig. 4 shows the proposed twin cross-shaped Hall sensor. In this design, we inject the current  $I_{bias}$  laterally in successive arms of the first cross-shaped Hall plate and drain identical current  $I_{bias}$  from the two successive arms of the second Hall plate. In this situation, the sensor structure is balanced with zero magnetic field, making null the output currents. An external magnetic field unbalances the sensor and provides two differential Hall currents,  $I_M$  and  $I_N$ , at the output nodes. If we fix the material and shape of a cross-shaped Hall plate, the differential Hall current is proportional to the external magnetic field ( $B_{\perp}$ ), biasing

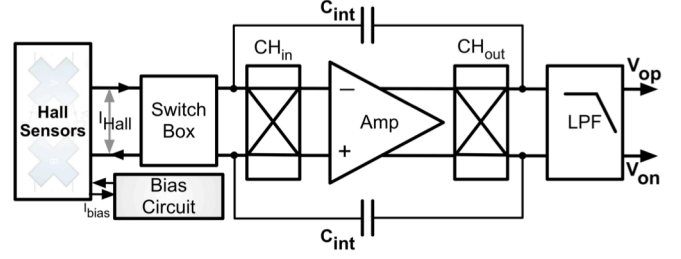


**Fig. 5.** A block diagram for the proposed Hall sensor microsystem. current of the Hall plate ( $I_{bias}$ ) and magnetic resistance coefficient ( $\beta$ ), which can be expressed as [12]

$$I_{Hall} = \frac{\beta B_{\perp} I_{bias}}{1 - (\beta B_{\perp})^2}, \quad (7)$$

where  $\beta$  is the magnetic resistance coefficient in the presence of a magnetic field. It is defined as

$$\beta = \frac{R_{(B)} - R_{(B=0)}}{R_{(B=0)} B_{\perp}}. \quad (8)$$

In Eq. (8)  $R_{(B=0)}$  and  $R_{(B)}$  refer to the Hall plate resistance in absence and presence of an external magnetic field  $B_{\perp}$ , respectively.

The output currents of each Hall plate,  $I_{H+}$  and  $I_{H-}$  in Fig. 4 are

$$I_{H+} = \frac{I_{bias}}{2} + \frac{I_{Hall}}{2}, \quad (9)$$

$$I_{H-} = \frac{I_{bias}}{2} - \frac{I_{Hall}}{2}. \quad (10)$$

For the used configuration, two Hall plates make two output currents,  $I_M$  and  $I_N$ , which are the difference of the output currents in each Hall plate. Finally, using Eq. (9) and Eq. (10), the sensor output currents are

$$I_N = I_{H+} - I_{H-} = I_{Hall}, \quad (11)$$

$$I_M = I_{H-} - I_{H+} = -I_{Hall}. \quad (12)$$

A standard system architecture of the proposed Hall sensor is shown in Fig. 5. It consists of two Hall sensors and a chain of dedicated electronic blocks. The main function of the front-end is to improve the sensitivity and decrease the residual offset. The front-end is made up of a chopper integrator amplifier, which acts as a current-to-voltage converter, and a switched capacitor filter, which offers low pass filtering.

#### IV. EXPERIMENTAL RESULTS

The proposed Hall sensor microsystem is fabricated in a standard 0.18- $\mu\text{m}$  CMOS process with 6 metals and 2 poly layers, as the microphotograph of fabricated chip illustrated in Fig. 6. Table I summarizes the microsystem performance for a bias current of 12  $\mu\text{A}$  and provides a comparison of this work with two other recently published CMOS Hall sensors.

The overall measured power consumption is about 110  $\mu$ W of which 54  $\mu$ W is consumed by the readout section. The sensor and the relevant switches for current spinning measured power consumption is approximately 55  $\mu$ W.

TABLE I. PERFORMANCE SUMMARY OF PROPOSED CMOS HALL SENSORS.

Specification	[13]	[14]	This Work
Year	2015	2016	2017
Technology	0.18 $\mu$ m	0.5 $\mu$ m	0.18 $\mu$ m
Chip Area	2500 $\times$ 3500 $\mu$ m <sup>2</sup>	1300 $\times$ 1300 $\mu$ m <sup>2</sup>	230 $\times$ 310 $\mu$ m <sup>2</sup>
Sensor Size	154 $\times$ 154 $\mu$ m <sup>2</sup>	300 $\times$ 280 $\mu$ m <sup>2</sup>	150 $\times$ 8 $\mu$ m <sup>2</sup>
Bias Current	1.4 mA	4.7 mA	12 $\mu$ A
Power Supply	5 V	5 V	1.8 V
Sensitivity	0.05 V/T	55 V/T	2400 V/A/mT
Power Consumption	-	-	110 $\mu$ W

## V. CONCLUSION

This paper serves as a proof of concept for the feasibility of using CMOS magnetic sensors for MMG. A magnetic Hall microsystem with two Hall sensors operating in the current-mode, able to provide differential currents at the output nodes was fabricated on a standard 0.18- $\mu$ m CMOS platform. The use of dedicated readout circuit with the integrated sensors will improve the signal-to-noise ratio and sensitivity. In this work, a low-noise chopper stabilized operational amplifier enabled the integration of the signal current and ensured appropriate voltage sensitivity. The use of the crossed-shaped Hall plates and a current-mode voltage output approach enabled current spinning technique for offset cancellation. Finally, by utilizing this chip, the pico-tesla bio-magnetic field can be converted to corresponding microvolt voltage signals. The overall measured offset, power consumption and the achieved voltage sensor sensitivity after the sensor frontend were promising and validated the effectiveness of integrated CMOS magnetic sensors for future screening of skeletal muscle activity with potential application in upper-limb prosthesis control.

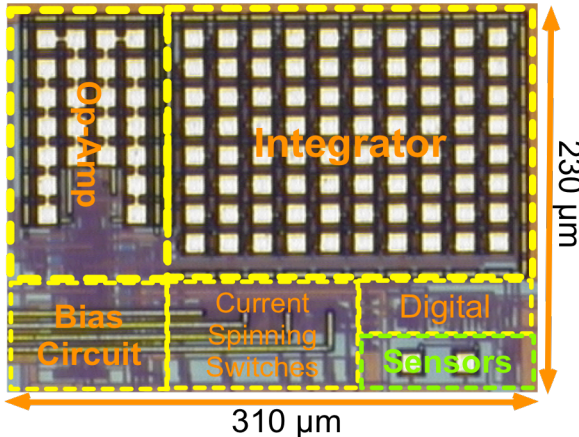


Fig. 6. The microphotograph of active zone of the fabricated chip, with highlighted main circuitual blocks. The chip occupies an active area of 300  $\times$  230  $\mu$ m<sup>2</sup>.

Having offered a potential architecture for wearable and implantable MMG, we acknowledge that measurement of such small MMG signals will remain a technical challenge from two angles:

1. There are considerable electromagnetic contaminations around our living environment but there are no off-the-shelf solutions for detection of MMG signals in non-magnetically shielded environments at body temperature.
2. There exist uniform background magnetic fields from the earth (e.g. geomagnetic field), which would lead to bio-sensor saturation [15]. Therefore, it would be a huge challenge to isolate the extremely weak bio-magnetic components of the measured signals in the low frequency domain (< 500Hz).

## REFERENCES

- [1] M. A. C. Garcia and O. Baffa, "Magnetic fields from skeletal muscles: A valuable physiological measurement?," *Front. Physiol.*, vol. 6, no. Aug, pp. 1–4, 2015.
- [2] D. Cohen and E. Givler, "Magnetomyography: Magnetic fields around the human body produced by skeletal muscles," *Appl. Phys. Lett.*, vol. 21, no. 3, pp. 114–116, 1972.
- [3] K. K. Parker and J. P. Wikswo, "A model of the magnetic fields created by single motor unit compound action potentials in skeletal muscle," *IEEE Trans. Biomed. Eng.*, vol. 44, no. 10, pp. 948–57, 1997.
- [4] R. Körber *et al.*, "SQUIDS in biomagnetism: a roadmap towards improved healthcare," *Supercond. Sci. Technol.*, vol. 29, no. 11, p. 113001, 2016.
- [5] J. Lenz and S. Edelstein, "Magnetic sensors and their applications," *IEEE Sens. J.*, vol. 6, no. 3, pp. 631–649, 2006.
- [6] J. M. van Egeraat, R. N. Friedman, and J. P. Wikswo, "Magnetic field of a single muscle fiber. First measurements and a core conductor model," *Biophys. J.*, vol. 57, no. 3, pp. 663–667, 1990.
- [7] A. Krasoulis, I. Kyranou, M. S. Erden, K. Nazarpour, and S. Vijayakumar, "Improved prosthetic hand control with concurrent use of myoelectric and inertial measurements," *J. Neuroeng. Rehabil.*, vol. 14, no. 1, p. 71, 2017.
- [8] A. Bilotti, G. Monreal, and R. Vig, "Monolithic magnetic Hall sensor using dynamic quadrature offset cancellation," *IEEE J. Solid-State Circuits*, vol. 32, no. 6, pp. 829–836, 1997.
- [9] H. Heidari, E. Bonizzoni, U. Gatti, and F. Maloberti, "A current-mode CMOS integrated microsystem for current spinning magnetic hall sensors," *Proc. - IEEE Int. Symp. Circuits Syst.*, pp. 678–681, 2014.
- [10] H. Heidari, E. Bonizzoni, U. Gatti, and F. Maloberti, "A 0.18- $\mu$ m CMOS current-mode hall magnetic sensor with very low bias current and high sensitive front-end," in *SENSORS, 2014 IEEE*, 2014, pp. 1467–1470.
- [11] H. Heidari, U. Gatti, and F. Maloberti, "Sensitivity characteristics of horizontal and vertical Hall sensors in the voltage-and current-mode," *2015 11th Conf. Ph.D. Res. Microelectron. Electron. PRIME 2015*, pp. 330–333, 2015.
- [12] H. Heidari, E. Bonizzoni, U. Gatti, and F. Maloberti, "A CMOS current-mode magnetic hall sensor with integrated front-end," *IEEE Trans. Circuits Syst. I Regul. Pap.*, vol. 62, no. 5, pp. 1270–1278, 2015.
- [13] J. Jiang and K. A. A. Makinwa, "A multi-path CMOS Hall sensor with integrated ripple reduction loops," in *Solid-State Circuits Conference (A-SSCC), 2015 IEEE Asian*, 2015, pp. 1–4.
- [14] T. Chang and K.-C. Juang, "CMOS hall sensor with reduced sensitivity drift by synchronous excitation calibration for wearable biomagnetic sensor in system-on-chip," in *SENSORS, 2016 IEEE*, 2016, pp. 1–3.
- [15] Z. Wang, M. Xu, X. Xu, and Z. Zhou, "Bio-magnetic sensor circuit design based on giant magneto-impedance effect," *2016 IEEE Int. Conf. Mechatronics Autom.*, pp. 2209–2214, 2016.